研 究 速 報

Estimating Solar Energy Flow to the Earth's Biosphere

地球生物圏への太陽エネルギーフローの推定

Dennis G. Dye*
デニス G ダイ

1. Introduction

Biological processes on Earth, with limited exceptions, are supported by the energy from the sun that is captured by plant organisms through the process of photoautotrophic primary production. The process utilizes photosynthetically active radiation (PAR, 400 – 700 nm), which contains approximately 45% of the energy in the total solar radiation incident at the Earth's surface. The portion of the PAR energy that becomes stored in the chemical bonds of plant biomass constitutes the basic energy reservoir for the planetary food web.

Primary production influences the state and functioning of the biosphere through physical linkages to the global biogeochemical, hydrological and nutrient cycles. Success in modeling and monitoring these processes depends in part on the availability of reliable global data on the magnitude and dynamics of incident and vegetation-absorbed PAR. This paper reports on results from an analysis of the spatial and temporal patterns of PAR and APAR performed using data derived using satellite remote sensing techniques.

2. Background

The amount of PAR energy absorbed by terrestrial vegetation (APAR, MJ m^{-2}) over a specified time interval t may be defined as

$$APAR_t = FAPAR_t \cdot S_t , \qquad (1)$$

where FAPAR is the fraction of incident PAR absorbed by the photosynthetic elements of the vegetation cover, and S is the total incident PAR (MJ m^{-2}). FAPAR is a measure of the capacity of the vegetation in the observed landscape to intercept and absorb incident PAR, and is closely related to green-leaf biomass and leaf area index (LAI). The S term defines the amount of PAR energy that is available for interception and absorption.

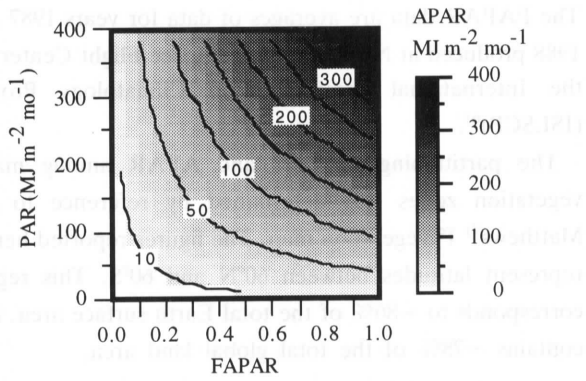

Fig. 1 Variation in APAR (contours and gray levels) as a function of monthly incident PAR and FAPAR.

The magnitudes of FAPAR and PAR at a given location and time determine the amount of energy diverted to primary production, and reflect the combined influences of vegetation cover and solar climate (Fig. 1). High incident PAR coincident with very low FAPAR (e.g. a low or mid-latitude desert) results in low APAR. Conversely, high incident PAR coincident with high FAPAR produces very high APAR (e.g, lush, irrigated croplands in an arid region). Because equal magnitudes of APAR can be achieved with different PAR-FAPAR combinations, global APAR patterns cannot be reliably predicted from knowledge of only FAPAR or only PAR.

3. Satellite Data Sources

PAR and FAPAR can be estimated and mapped on a

*Dept. of Building and Civil Engineering, Institute of Industrial Science, University of Tokyo

global basis using recent satellite remote sensing techniques[1]. Measurements of 370 nm reflectivity from the Nimbus-7 Total Ozone Mapping Spectrometer (TOMS) are well-suited for estimating incident PAR[2]. Field and modeling studies have shown that remotely sensed measurements of the normalized difference vegetation index (NDVI) are good predictors of FAPAR[3].

This analysis employs two existing satellite-derived data sets of monthly PAR and FAPAR, each providing global or near-global coverage with 1° spatial resolution. The PAR data were produced in earlier work[4),5] using the method of Eck and Dye[2] and cover the 11 years from 1979 to 1989. The FAPAR data are averages of data for years 1987 and 1988 produced at NASA Goddard Space Flight Center for the International Satellite Land Climatology Project (ISLSCP)[6].

The partitioning of PAR and APAR among major vegetation zones was determined by reference to the Matthews[7] 1° vegetation map. The figures reported herein represent latitudes between 60°N and 60°S. This region corresponds to ~86% of the total Earth surface area, and contains ~78% of the total global land area.

4. Incident PAR

In the absence of variable clouds and aerosols in the atmosphere, the spatial pattern of PAR at the Earth's surface would follow the top-of-the-atmosphere pattern, i.e. decreasing in a smooth gradient from the tropics to the poles as influenced by seasonality in sun-earth geometry. The interaction of clouds and aerosols with this potential pattern results in the observed pattern of annual PAR (Fig. 2).

In equatorial regions, perennially abundant cloud cover dramatically reduces PAR at the surface relative to the potential amount. The largest annual amounts of PAR are received at subtropical latitudes in zones characterized by atmospheric subsidence. These zones contain major desert regions of the globe.

The 11-year mean of annual total incident PAR (60°N – 60°S) is computed as 1.26×10^6 EJ (Table 1). This value represents the maximum energy available annually in the biosphere that can support photosynthesis and primary production. Of this total amount, 9.17×10^5 EJ (73%) is incident on water bodies (oceans, seas, major lakes), and 3.42×10^5 EJ (27%) is incident on land surfaces. The key factors that influence this partitioning are the proportion and latitudinal distribution of land and ocean surface areas, and land-ocean differences in cloud cover distribution and seasonality.

The time series of annual total global PAR shows no strong decadal trend (Fig. 3). The year 1982, however, is marked by an anomalous reduction in PAR, which is particularly pronounced in the northern hemisphere (Fig. 3). At least two events of global significance occurred in 1982 that may account for this anomalous reduction. One is the onset of a major El Niño/Southern Oscillation event that carried over into 1983. ENSO conditions are characterized

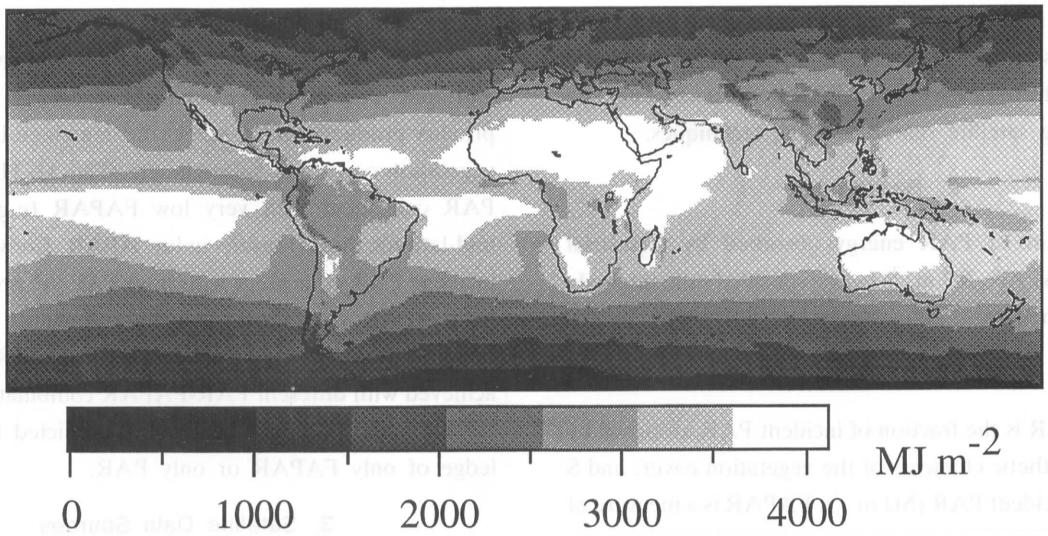

Fig. 2 Mean of annual total PAR for years 1979 to 1989. Estimates are based on 370 nm reflectivity data from Nimbus-7 TOMS.

Table 1 Satellite-based estimates of annual total PAR and APAR for major surface cover types in latitudes 60 N–60 S. Mean values are for the 1979–1989 period.

Vegetation/Surface Type	Area (km^2)	PAR Mean (J)	APAR Mean (J)
Water (Oceans, Seas, Lakes)	3.28E+08	9.17E+23	
Forests, Woodlands	5.53E+07	1.44E+23	7.26E+22
Grassland, Shrubland, & Non-Woody Veg.	4.84E+07	1.44E+23	3.48E+22
Desert and Ice	1.55E+07	5.41E+22	2.70E+21
TOTAL, LAND ONLY	1.19E+08	3.42E+23	1.10E+23
TOTAL , LAND & WATER	4.47E+08	1.26E+24	

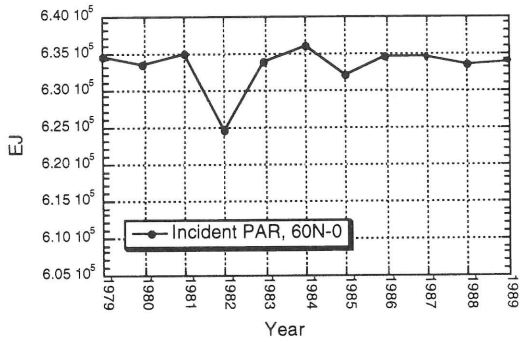

Fig. 3 Time series (1979–1989) of annual total surface-incident PAR for 0 to 60 N latitude (northern hemisphere). The value for 1982 corresponds to an approximate 1.7% reduction in total incident PAR.

by regional changes in cloudiness, notably a shift in cloud cover (and sea surface temperature) from the western to the eastern tropical Pacific Ocean. Another noteworthy event in 1982 was the eruption of Mexico's El Chichón volcano, which released a large volume of aerosol material into the atmosphere and reduced the transmissivity of the atmosphere.

5. Terrestrial APAR

Owing to its dependence on vegetation cover as well as on incident PAR, the spatial pattern of annual APAR for global land areas (Fig. 4) diverges markedly from the PAR pattern (Fig. 2). At the annual time scale, the largest values occur in the tropical rainforest zones where FAPAR and PAR are both perennially high. Low values of APAR occur in desert or sparsely vegetated regions where available PAR may be high but, in the absence of water, little or no vegetation can be sustained to utilize it. The low APAR values at high latitudes are attributable to limitations by both available PAR (latitude effect) and FAPAR (tempera-

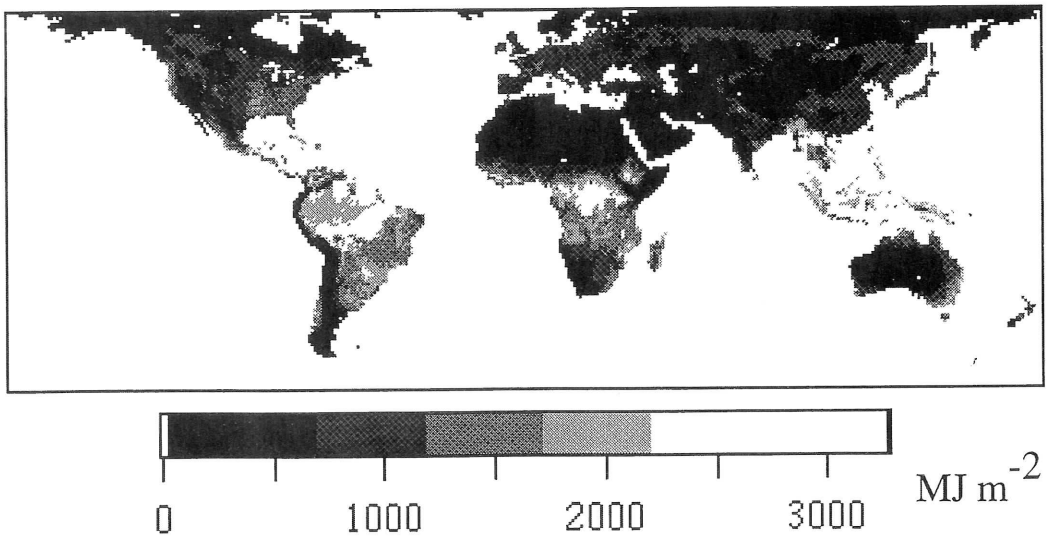

Fig. 4 Mean (1979–1989) of annual total vegetation-absorbed photosynthetically active radiation (APAR) for land areas.

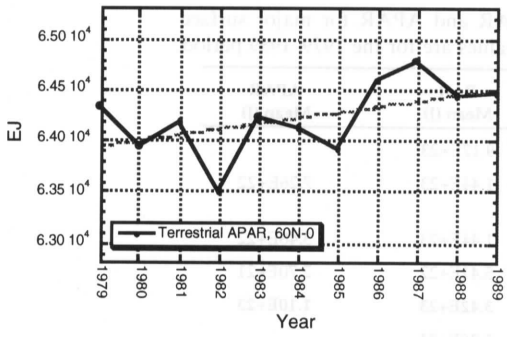

Fig. 5 Time series (1979–1989) of terrestrial APAR for northern hemisphere land areas (60 N–0). The dashed line indicates the line of least-squares from linear regression.

ture restrictions on photosynthetic activity and vegetation canopy development)

The analysis indicates terrestrial vegetation between 60°N and 60°S latitudes intercepts and absorbs an average of 1.10 $\times 10^5$ EJ PAR annually (Table 1). This amount corresponds to 8.8% of the global total incident PAR and 32.3% of the total terrestrial incident PAR in this latitude zone. Grassland/shrubland and forest zones, though differing in surface area, receive equal amounts of PAR energy (Table 1). The annual amount of PAR that is captured by vegetation, however, is more than 50% greater in forest zones than in grassland/shrubland zones.

The time series of northern hemisphere annual total terrestrial APAR (60°N – 0°) exhibits notable interannual variation (Fig. 5). The influence of the ENSO and possibly El Chichón-related reduction in incident PAR on terrestrial APAR in 1982 is evident. A decadal-scale trend toward increasing terrestrial APAR is also detectable. Based on line of least squares from linear regression, northern hemisphere terrestrial APAR increased at an average rate of 57.56 EJ y^{-1}, or approximately 0.9% of the 11-year mean northern hemisphere APAR mean value of 6.42 $\times 10^4$ EJ y^{-1}.

6. Summary

Global satellite estimates of annual incident and terrestrial vegetation-absorbed photosynthetically active radiation (PAR, 400–700 nm) were evaluated for the 11 years from 1979 to 1989. The results constitute a first satellite-based examination of the global receipt and biological diversion of photosynthetically active radiation. The observed patterns define the energy basis for global primary production and biospheric functioning.

A 1.7% reduction in northern hemisphere (60°N–0°) incident PAR in 1982 is attributed to changes in cloud amount and distribution associated with El Niño-Southern Oscillation conditions and possibly aerosols from the 1982 El Chichón volcanic eruption. The observed interannual variations and trends, if confirmed, may have significant influence on global patterns of primary production. This influence may occur directly through fluctuations in the energy flow to photosynthesis, and indirectly through relations to other climatic variables, such as temperature and precipitation, that influence growth and production.

Research in progress is directed toward providing additional validation and refinement of the PAR and FAPAR estimates, and applying the data in a mechanistic model to evaluate the spatial and temporal patterns of terrestrial primary productivity. In future research, the analysis will be extended to examine PAR absorbed by ocean primary producers. (Manuscript received, September 12, 1995)

References

1) Dye, D.G., and Goward, S.N., 1993, Absorption of photosynthetically active radiation by global land vegetation in August 1984. International Journal of Remote Sensing, 14(18):3361–3364.
2) Eck, T.F., and Dye, D.G., 1991. Satellite estimation of incident photosynthetically active radiation using ultraviolet reflectance. Remote Sensing of Environment, 38:135–146.
3) Goward, S.N., and Huemmrich, K.F., 1992. Vegetation canopy PAR absorptance and the normalized difference vegetation index: An assessment using the SAIL model. Remote Sensing of Environment, 39:119–140.
4) Dye, D.G., 1992. Satellite estimation of the global distribution and interannual variability of photosynthetically active radiation. Ph.D. dissertation, University of Maryland, College Park.
5) Dye, D. G., and Shibasaki, R., 1995, Intercomparison of global PAR data sets. Geophysical Research Letters, 22(15):2013–2016.
6) Sellers, P.J., S.O. Los, C.J. Tucker, C.O. Justice, D.A. Dazlich, G.J. Collatz, and D.A. Randall, 1994. A global 1 by 1 degree NDVI data set for climate studies. Part 2: The generation of global fields of terrestrial biophysical parameters from the NDVI. International Journal of Remote Sensing, 15(17):3519–3545.
7) Matthews, E., 1983. Global vegetation and land use: New high-resolution data bases for climate studies, J. Clim. Appl. Meteor., 22, 474–487.